

Distributed goal assignment strategy for improving leader-following formation control performance

Yun Ho Choi^a, Doik Kim^{a,*}

^a*Center for Intelligent & Interactive Robotics Research, Korea Institute of Science and Technology, 5, Hwarang-ro 14-gil, Seongbuk-gu, Seoul, 02792, South Korea*

Abstract

This paper investigates a distributed goal assignment problem in leader-following formation control of second-order multi-agent systems. It is assumed that each agent can communicate with nearby agents within the communication range and the leader information is only available to a subset of agents. Compared with existing formation control schemes addressing the goal assignment issue, the main contribution of this paper is to construct a novel distributed assignment strategy allotting appropriate goal positions of agents in the leader-following formation control framework. Based on the rigorous analysis using the Lyapunov stability theory, the enhancement of the control performance is proved via the proposed assignment strategy. To demonstrate the effectiveness of our theoretical results, two examples including multiple quadrotors are simulated.

Keywords: Distributed goal assignment, goal exchange, leader-following formation control, multi-agent systems.

1. Introduction

Distributed coordination of multi-agent systems has attracted considerable attention from multidisciplinary areas owing to its broad applications such as scheduling of automated highway systems, attitude alignment of satellites, cooperative transport, and so on [1, 2]. One of the fundamental problems of coordination of multi-agent systems is formation control. The aim of formation control is to design an appropriate control algorithm such that agents form a predefined geometrical shape. There are a lot of formation control results using different methodologies such as

*Corresponding author.

Email address: doikkim@kist.re.kr (Doik Kim)

behavior-based [3], virtual structure [4], and leader-following approaches [5]. Among those methodologies, the leader-following approach has been widely employed because of its simplicity and reliability [5, 6, 7, 8]. In this approach, a predefined formation shape is specified by the relative positions between a referenced agent called a leader and other agents called followers. Therefore, each follower is controlled to keep the pre-specified relative position from the leader. For a group of tractor-trailer systems, an adaptive leader-following formation controller using neural networks was designed in [6]. In [7] and [8], leader-following control schemes were developed for autonomous underwater vehicles without the leader velocity, and mobile robots with docking systems considering the battery failure and maneuverability on rough terrain, respectively. However, these studies [6, 7, 8] assumed that the leader communicates with all followers which limits their applicability because the real multi-robot systems have a limited communication range. To address this problem, a number of researchers have developed leader-following formation control schemes in the presence of limited leader information under the distributed communication network. In [9, 10], formation control and collision avoidance problems were handled simultaneously by adopting the artificial potential function approach. Recently, time-varying formation trackers were designed considering mismatched disturbances [11] or switching communication topology [12]. For practical applications of leader-following formation control approaches, various robotic systems were handled such as mobile robots [13, 14], underwater vehicles [15, 16], surface vehicles [17], and quadrotors [18]. Nevertheless, in the existing leader-following formation control schemes [9, 10, 11, 12, 13, 14, 15, 16, 17, 18], the goal assignment issue allotting appropriate goal positions for followers was not investigated where the goal indicates the desired relative position with respect to the leader. Namely, the goals of followers in [9, 10, 11, 12, 13, 14, 15, 16, 17, 18] are not allowed to be changed which leaves room for the development of assignment strategy in the leader-following formation control field.

In coordinated control of multi-agent systems, goal assignment plays a key role because it can reduce the time required to reach the goal position. From the practical point of view, this advantage becomes more significant when the scale of the team of agents is huge like the drone show. Thus, substantial efforts have been devoted to resolving the goal assignment issue. Centralized assignment strategies were suggested to minimize the sum of the distance traveled or the sum of the squared distance traveled by agents in [19, 20]. To improve scalability, distributed goal assignment strategies have been developed recently. In [21], a multiple Lyapunov function method was used to assign goals of agents as well as to generate safe trajectories in a distributed manner. In [22], a distributed algorithm assigning goals and creating a

collision-free path to the goals was presented where the path is given by a sequence of nodes of the grid-based environment. Despite this success, the goal positions considered in [21, 22] are defined as absolute positions, and thus the existing assigning methods cannot be applied to the leader-following formation control where goals of followers are given by relative positions from the leader. Moreover, their approaches are only applicable to first-order multi-agent systems. In [23], a leader-following formation control problem with distributed goal assignment was investigated. The main procedure of the goal assignment algorithm in [23] is to select two agents and exchange their goals if an error under the current goals is bigger than that under the exchanged goals. Recently, this work is extended to second-order systems [24]. However, these works [23, 24] suffered from the fact that all the followers should know the leader information. Thus, the centralized communication with the center node being the leader for leader-following multi-agent systems should be available. From the practical point of view, the centralized communication is not available for some robots with limited communication range and it can encounter a significant bottleneck on the central node as the number of followers increases. That is, the strategies in [23, 24] cannot deal with the assignment problem of large-scale multi-robot systems under the distributed communication network. There is a recent formation control approach with distributed goal assignment was presented in [25]. However, since this assignment strategy was developed based on the distance-based formation control framework, we cannot apply this strategy to the leader-following formation control framework.

Motivated by these observations, this paper aims to develop a novel distributed goal assignment strategy for leader-following formation control. We assume that the leader information is only available for a fraction of second-order followers and followers can communicate with nearby agents within their communication range. Compared with existing related literature, the major contribution of this paper is three-fold:

(C1) This is the first attempt to address the goal assignment issue in leader-following formation control with limited leader information. That is, the goals of followers are assigned properly using an online goal assignment strategy different from the previous leader-following formation control schemes with fixed goals [9, 10, 11, 12, 13, 14, 15, 16, 17, 18].

(C2) In contrast to the centralized communication-based control and assignment scheme [23, 24], the proposed controller and assignment algorithm can be performed under the distributed communication network by designing a distributed leader estimator.

(C3) To reflect the distributed communication in goal assignment, a novel as-

signment strategy exchanging not only the goal positions but also the neighbors is developed. Besides, it is rigorously proved that the formation control performance is improved using the proposed assignment strategy.

The remainder of this paper is structured as follows. In Section 2, some preliminaries are given and the control problem is formulated. In Section 3, a distributed estimator and a controller are derived and the asymptotic stability is analyzed. Section 4 introduces a new goal assignment algorithm and the improved control performance is revealed using the proposed assignment algorithm. To illustrate the feasibility of our theoretical results, a group of multiple quadrotors are simulated in Section 5. Conclusions are drawn in Section 6.

2. Preliminaries and problem formulation

2.1. Second-order multi-agent systems

We consider the formation control problem of a group of agents in \mathbb{R}^d consisting of a virtual leader and N followers with $d = 2, 3$. Each follower is modeled as follows:

$$\begin{aligned}\dot{p}_i(t) &= v_i(t) \\ \dot{v}_i(t) &= u_i(t)\end{aligned}\tag{1}$$

where $i = 1, \dots, N$, $p_i(t)$, $v_i(t)$, and $u_i(t)$ denote the position, velocity, and control input of agent i , respectively. In this paper, the leader's position is defined as $p_0(t)$ which is independent of followers.

Assumption 1. Let the velocity and acceleration of the leader be $v_0(t) \triangleq \dot{p}_0(t)$ and $u_0(t) \triangleq \ddot{p}_0(t)$. Then, the acceleration and its derivative is bounded as $\|u_0(t)\| \leq C_{u,0}$ and $\|\dot{u}_0(t)\| \leq C_{u,1}$ where $C_{u,0}$ and $C_{u,1}$ are positive constants.

2.2. Communication environment

This section introduces the communication setup for the considered multi-agent system (1).

Assumption 2. Followers can communicate with nearby followers that are within their communication range R .

Assumption 3. Leader information $p_0(t)$, $v_0(t)$, and $u_0(t)$ are only available for a fraction of followers.

To represent the communication among agents, we consider a graph $\mathcal{G}(\mathcal{V}, \mathcal{E})$ where $\mathcal{V} = \{0, 1, \dots, N\}$ and $\mathcal{E} \subseteq \mathcal{V} \times \mathcal{V}$; node 0 indicates the leader and nodes $1, \dots, N$ denote the followers. There exist undirected edges $(i, j) \in \mathcal{E}$ if $\|p_i(t) - p_j(t)\| \leq R$ where $p_i(t)$ and $p_j(t)$ denote the positions of follower i and follower j , respectively, and $j \neq i$. Different from the edges among followers, the edges from the leader to a subset of the followers are regarded as directed edges because the leader has an independent motion.

In this paper, a distinct graph $\bar{\mathcal{G}}(\mathcal{V}, \bar{\mathcal{E}})$ is introduced to characterize the controller network where $\bar{\mathcal{E}} \subseteq \mathcal{E}$ [26]. This graph defines the set of information required in the local control system. Since the communication among agents is range-limited, $\bar{\mathcal{G}}(\mathcal{V}, \bar{\mathcal{E}})$ is a subgraph of $\mathcal{G}(\mathcal{V}, \mathcal{E})$. That is, $\bar{\mathcal{E}} \subseteq \mathcal{E}$.

To describe the controller network among followers, we consider an undirected graph $\bar{\mathcal{G}}_F(\mathcal{V}_F, \bar{\mathcal{E}}_F)$ where $\mathcal{V}_F = \{1, \dots, N\}$ and $\bar{\mathcal{E}}_F \subset \bar{\mathcal{E}}$. Let an adjacency matrix be $A_F = [a_{ij}] \in \mathbb{R}^{N \times N}$ for $\bar{\mathcal{G}}_F$ and a leader adjacency matrix be $B = \text{diag}\{b_1, \dots, b_N\} \in \mathbb{R}^{N \times N}$ associated with $\bar{\mathcal{G}}$ where $a_{ii} = 0$, $a_{ij} = a_{ji}$, $a_{ij} = 1$ if $(j, i) \in \bar{\mathcal{E}}_F$, $a_{ij} = 0$ otherwise, and $b_i = 1$ if $(0, i) \in \bar{\mathcal{E}}$ and $b_i = 0$ otherwise. From A_F , the Laplacian matrix $L_F = [l_{ij}] \in \mathbb{R}^{N \times N}$ is defined as $l_{ii} = \sum_{j \neq i} a_{ij}$ and $l_{ij} = -a_{ij}$ where $j \neq i$. According to the two graphs $\mathcal{G}(\mathcal{V}, \mathcal{E})$ and $\bar{\mathcal{G}}(\mathcal{V}, \bar{\mathcal{E}})$, the set of neighbors \mathcal{N}_i and $\bar{\mathcal{N}}_i$ are defined as $\mathcal{N}_i = \{j \mid (i, j) \in \mathcal{E}\}$ and $\bar{\mathcal{N}}_i = \{j \mid (i, j) \in \bar{\mathcal{E}}\}$, respectively where $i = 1, \dots, N$. For the control graph $\bar{\mathcal{G}}$, we use the following assumption.

Assumption 4. [27] The graph $\bar{\mathcal{G}}$ has a spanning tree with the root node being the leader. That is, there exist paths from the leader to all followers where each path is defined as a sequence of ordered edges of the form $(0, i_1), (i_1, i_2), \dots, (i_k, i)$ with $i = 1, \dots, N$.

Fig. 1(a) and 1(b) illustrate an example of the communication graph $\mathcal{G}(\mathcal{V}, \mathcal{E})$ and the control graph $\bar{\mathcal{G}}(\mathcal{V}, \bar{\mathcal{E}})$, respectively, satisfying Assumptions 2, 3, and 4. From this figure, it is seen that the control graph in Fig. 1(b) is a subgraph of the communication graph in Fig. 1(a).

2.3. Problem formulation

In this paper, goal positions G_i , $i = 1, \dots, N$, are defined as the relative desired positions with respect to the leader to form the target shape. For the goal positions, we use the following assumption.

Assumption 5. [21] Each agent can converge to any goal positions with respect to the leader. That is, the goal positions are interchangeable.

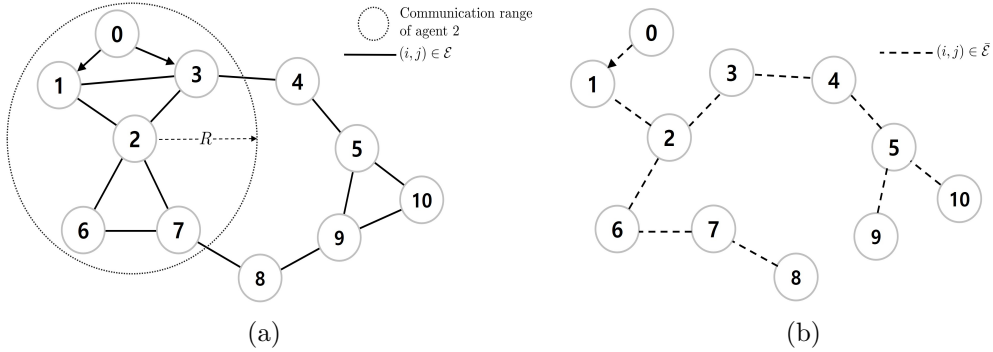


Figure 1: Example of two network topologies (a) $\mathcal{G}(\mathcal{V}, \mathcal{E})$ (b) $\bar{\mathcal{G}}(\mathcal{V}, \bar{\mathcal{E}})$.

Problem 1. Consider the leader-following multi-agent systems consisting of one leader and N followers (1) under Assumptions 2–5. Our problem is designing distributed control laws to form the target formation and developing an online goal assignment strategy exchanging goals of the agents to improve the leader-following formation control performance.

Remark 1. Different from the existing distributed leader-following formation control schemes [9, 10, 11, 12, 13, 14, 15, 16, 17, 18] with fixed goal positions, we consider interchangeable goals as stated in Assumption 5. In [21, 22], distributed goal assignment algorithms were presented for multi-agent systems, but those cannot be used for Problem 1 because there was no leader and only the first-order agents were handled. Even though leader-following control schemes with goal assignment were proposed in [23, 24], these necessitate the network connection from the leader to all followers. In conclusion, Problem 1 is not solved by the previous related literature [9, 10, 11, 12, 13, 14, 15, 16, 17, 18, 21, 22, 23, 24].

3. Distributed formation controller Design

3.1. Leader estimator design

Motivated by the work of Liang et al. [28], a distributed leader estimator for each follower is derived as follows:

$$\begin{aligned}
\dot{\hat{p}}_{i,0} &= \hat{v}_{i,0} \\
\dot{\hat{v}}_{i,0} &= \hat{u}_{i,0} \\
\dot{\hat{u}}_{i,0} &= -\gamma_{i,1} \left(\sum_{j=1}^N \bar{a}_{F,ij} (\hat{p}_{i,0} - \hat{p}_{j,0}) + \bar{b}_i (\hat{p}_{i,0} - p_0) \right) \\
&\quad - \gamma_{i,2} \left(\sum_{j=1}^N \bar{a}_{F,ij} (\hat{v}_{i,0} - \hat{v}_{j,0}) + \bar{b}_i (\hat{v}_{i,0} - v_0) \right) \\
&\quad - \gamma_{i,3} \left(\sum_{j=1}^N \bar{a}_{F,ij} (\hat{u}_{i,0} - \hat{u}_{j,0}) + \bar{b}_i (\hat{u}_{i,0} - u_0) \right)
\end{aligned} \tag{2}$$

where $i = 1, \dots, N$, $\gamma_{i,1}, \gamma_{i,2}, \gamma_{i,3} > 0$ are positive constants denoting the estimator gains, and $\hat{p}_{i,0}$, $\hat{v}_{i,0}$, and $\hat{u}_{i,0}$ are the estimated leader position, velocity, and acceleration, respectively.

Let us define local estimation errors $\tilde{p}_{i,0} = \hat{p}_{i,0} - p_0$, $\tilde{v}_{i,0} = \hat{v}_{i,0} - v_0$, and $\tilde{u}_{i,0} = \hat{u}_{i,0} - u_0$. Then, we get

$$\begin{aligned}
\dot{\tilde{p}}_0 &= \tilde{v}_0 \\
\dot{\tilde{v}}_0 &= \tilde{u}_0 \\
\dot{\tilde{u}}_0 &= -\gamma_1 ((\bar{L}_F + \bar{B}) \otimes I_d) \tilde{p}_0 - \gamma_2 ((\bar{L}_F + \bar{B}) \otimes I_d) \tilde{v}_0 \\
&\quad - \gamma_3 ((\bar{L}_F + \bar{B}) \otimes I_d) \tilde{u}_0 - 1_N \otimes \dot{u}_0
\end{aligned} \tag{3}$$

where $\tilde{p}_0 = [\tilde{p}_{1,0}^\top, \dots, \tilde{p}_{N,0}^\top]^\top \in \mathbb{R}^{dN}$, $\tilde{v}_0 = [\tilde{v}_{1,0}^\top, \dots, \tilde{v}_{N,0}^\top]^\top \in \mathbb{R}^{dN}$, $\tilde{u}_0 = [\tilde{u}_{1,0}^\top, \dots, \tilde{u}_{N,0}^\top]^\top \in \mathbb{R}^{dN}$, I_d is the $d \times d$ identity matrix, $\bar{L}_F \in \mathbb{R}^{N \times N}$ is the Laplacian matrix associated with $\bar{\mathcal{G}}_F$, $\bar{B} = \text{diag}\{\bar{b}_1, \dots, \bar{b}_N\}$, 1_N is N -vector of ones, $\gamma_j = \text{diag}\{\gamma_{j,1}, \dots, \gamma_{j,N}\}$ with $j = 1, 2, 3$, and \otimes indicates the Kronecker product.

Consider a vector $q = [\tilde{p}_0^\top, \tilde{v}_0^\top, \tilde{u}_0^\top]^\top \in \mathbb{R}^{3dN}$ and $H \triangleq (\bar{L}_F + \bar{B}) \otimes I_{d \times d}$. Then, the time derivative of \dot{q} using (3) is expressed by

$$\dot{q} = A_1 q + A_2 \tag{4}$$

where

$$A_1 = \begin{bmatrix} 0_{dN \times dN} & I_{dN \times dN} & 0_{dN \times dN} \\ 0_{dN \times dN} & 0_{dN \times dN} & I_{dN \times dN} \\ -\gamma_1 H & -\gamma_2 H & -\gamma_3 H \end{bmatrix} \in \mathbb{R}^{3dN \times 3dN}, \quad A_2 = \begin{bmatrix} 0_{dN} \\ 0_{dN} \\ -1_N \otimes \dot{u}_0 \end{bmatrix} \in \mathbb{R}^{3dN}$$

Owing to Assumption 4, H is positive definite [27], and thus A_1 is a stable matrix since γ_i , $i = 1, 2, 3$, are positive definite. Therefore, for any matrix $Q > 0$, there exists a positive definite matrix $P > 0$ satisfying Lyapunov equation $A_1^\top P + P A_1 = -Q$. Following the procedure of Section 3.3 in [28] and using the practical stability concept, we can easily ensure the uniformly ultimately boundedness of the estimation errors. Note that the estimator (2) can be replaced by other estimators presented in cooperative control problems of multi-agent systems with a leader such as the finite-time estimator in [29] or the fixed-time estimator in [30].

3.2. Controller design via backstepping technique

An auxiliary variable p_i^* is considered to indicate the goal position assigned to the i th follower. Note that the initial value of p_i^* is set to G_i (i.e., $p_i^*(0) = G_i$) for $i = 1, \dots, N$ but it could be varied along the goal assignment mechanism which will be shown in the next section. To design the local controller, we use the backstepping technique [31]. Then, two control error surfaces using the estimate leader position are defined as

$$\begin{aligned} e_{i,1} &= p_i - \hat{p}_{i,0} - p_i^* \\ e_{i,2} &= v_i - \zeta_i \end{aligned} \quad (5)$$

where $i = 1, \dots, N$ and ζ_i indicates the virtual controller of the i th follower.

According to the recursive design procedure of backstepping technique, the local virtual and actual controllers are derived as follows:

$$\zeta_i = -k_{i,1}e_{i,1} + \hat{v}_{i,0} \quad (6)$$

$$u_i = -k_{i,2}e_{i,2} - e_{i,1} + \dot{\zeta}_i \quad (7)$$

where $k_{i,1}, k_{i,2} > 0$ are control gains.

To analyze the closed-loop stability, let us consider a Lyapunov function as follows:

$$V = \frac{1}{2}e_1^\top e_1 + \frac{1}{2}e_2^\top e_2 \quad (8)$$

with $e_1 = [e_{1,1}^\top, \dots, e_{N,1}^\top]^\top$ and $e_2 = [e_{1,2}^\top, \dots, e_{N,2}^\top]^\top$. On the other hand, applying (6) and (7) into the derivatives of $e_{i,1}$ and $e_{i,2}$, we get

$$\begin{aligned} \dot{e}_{i,1} &= -k_{i,1}e_{i,1} + e_{i,2}, \\ \dot{e}_{i,2} &= -k_{i,2}e_{i,2} - e_{i,1}. \end{aligned} \quad (9)$$

Then, the time derivative of V is derived as follows:

$$\dot{V} = -e_1^\top k_1 e_1 - e_2^\top k_2 e_2 \quad (10)$$

where $k_1 = \text{diag}\{k_{1,1}, \dots, k_{N,1}\} \otimes I_d$ and $k_2 = \text{diag}\{k_{1,2}, \dots, k_{N,2}\} \otimes I_d$. By letting $k_m \triangleq \min_{i=1, \dots, N, j=1, 2} \{k_{i,j}\}$, the inequality $\dot{V} \leq -2k_m V$ holds. Consequently, the asymptotic convergence of the error surfaces $e_{i,1}$ and $e_{i,2}$, $i = 1, \dots, N$, is ensured based on the Lyapunov stability theory. Now, let us define the global formation error $\delta_i = p_i - p_0 - p_i^*$ of the i th follower. From the definition of $e_{i,1}$ and $\tilde{p}_{i,0}$, we get $\delta_i = e_{i,1} + \tilde{p}_{i,0}$. Since $\tilde{p}_{i,0}$ is uniformly bounded from Section 3.1 and $e_{i,1}$ converges to zero, the global formation error δ_i converges to nearby zero regarding to the magnitude of $\tilde{p}_{i,0}$. Therefore, we can conclude that the desired formation shape is achieved practically.

Remark 2. The guideline of the selecting the design parameters of the estimator and the controller is listed as follows: (i) increasing the estimator gains $\gamma_{i,1}$, $\gamma_{i,2}$, $\gamma_{i,3}$, $i = 1, \dots, N$, helps to increase the minimum eigenvalue of Q , which reduces the ultimate boundedness of the local estimation errors; (ii) increasing $k_{i,1}$ and $k_{i,2}$ improves the convergence speed of the local formation errors $e_{i,1}$.

4. Distributed goal assignment strategy

In order to improve the leader-following formation control performance, this section investigates an online distributed goal assignment problem by assigning proper goals for followers. In [23, 24], goal assignment strategies were suggested where the goal positions of two selected agents are swapped whenever a sum of the formation errors decreases along with the goal exchange. However, the assignment procedure in [23, 24] cannot be applied to our formation control problem because it requires that all followers can access the information of the leader. This condition is available only if the leader communicates with all followers or the leader information is pre-programmed in all followers. However, the pre-programmed approach is of low flexibility to the update of the leader signal in practice. Therefore, the previous strategies presented in [23, 24] were based on the centralized communication with the center node being the leader as displayed in Fig. 2(a). In contrast, we consider the distributed communication network determined by the communication range and the limited leader information as shown in 2(b), which is common in the conventional leader-following formation control schemes [9, 10, 11, 12, 13, 14, 15, 16, 17, 18]. The distributed network in Fig. 2(b) is more preferable since centralized communication can encounter a significant bottleneck on the central node as the number of agents increases. Recently, a distributed goal assignment approach was presented in [25] but its approach is developed in the sense of distance-based formation control and only the first-order agents were handled.

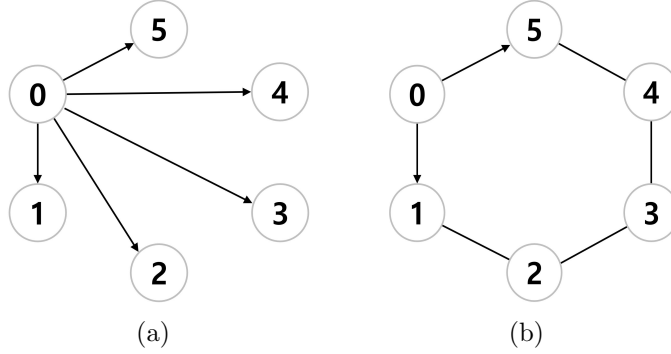


Figure 2: Comparison of the communication graph for the same hexagon one leader and five followers (a) \mathcal{G} in [23] (b) \mathcal{G} in the proposed control scheme.

Similar to [23, 24], in the proposed goal assignment procedure, two agents are selected and their goal positions are exchanged if a condition is satisfied. However, since the communication range is limited, we should exchange agents' neighbors $\bar{\mathcal{N}}_i$ associated with the control graph $\bar{\mathcal{G}}$ as well as their goal positions. The spanning tree condition in Assumption 4 is referred as a basic assumption in the previous leader-following control schemes [9, 10, 11, 12, 13, 14, 15, 16, 17, 18], but this assumption is normally based on the non-exchangeable goals. Therefore, Assumption 4 may not be guaranteed if agents' goals are exchanged in the presence of the limited communication range. To handle this issue, we propose an assignment strategy including the update of the set of their neighbors $\bar{\mathcal{N}}_i$ associated with the control graph $\bar{\mathcal{G}}$. To represent this transition, we use time-dependent variables $\mathcal{N}_i(t)$, $p_i^*(t)$, and $\bar{\mathcal{N}}_i(t)$. Let agents α and β be the selected two agents in the assignment strategy. Then, a basic assumption of the proposed assignment strategy is given as follows:

Assumption 6. For agents α and β , it holds that $\bar{\mathcal{N}}_\alpha(t) - \{\beta\} \subset \mathcal{N}_\beta(t)$ and $\bar{\mathcal{N}}_\beta(t) - \{\alpha\} \subset \mathcal{N}_\alpha(t)$.

Remark 3. Assumption 6 means that one of the two selected agents can get the information of not only its neighbors but also the other's neighbors defined in the control graph $\bar{\mathcal{G}}(t)$. This assumption is mandatory in the proposed assignment process to maintain the spanning tree condition of $\bar{\mathcal{G}}(t)$ (i.e., Assumption 4) because the goal exchange of two agents basically leads to the change of $\bar{\mathcal{G}}(t)$ by updating their neighbors $\bar{\mathcal{N}}_i(t)$. For a better understanding of Assumption 6, let us see Fig. 3 illustrating the communication and control graphs of seven agents. Note that

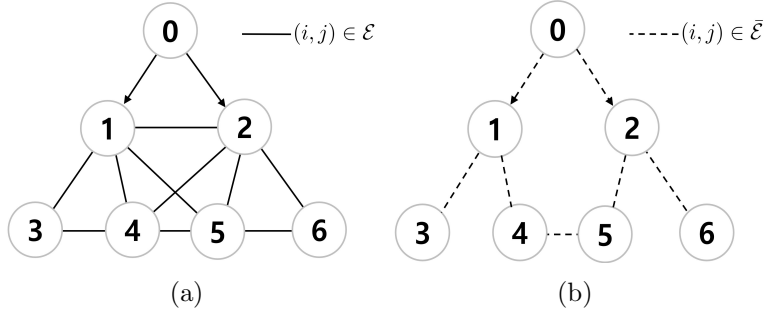


Figure 3: Communication and control graphs satisfying Assumption 6 for $\alpha = 4$ and $\beta = 5$ (a) $\mathcal{G}(\mathcal{V}, \mathcal{E})$ (b) $\bar{\mathcal{G}}(\mathcal{V}, \bar{\mathcal{E}})$.

Assumption 6 is satisfied for agents 4 and 5 because

$$\begin{aligned} \bar{\mathcal{N}}_4(t) &= \{1, 5\}, & \mathcal{N}_4(t) &= \{1, 2, 3, 5\}, \\ \bar{\mathcal{N}}_5(t) &= \{2, 4\}, & \mathcal{N}_5(t) &= \{1, 2, 4, 6\}. \end{aligned} \quad (11)$$

Using Assumption 6, the proposed distributed online goal assignment algorithm is presented in Algorithm 1. Simply, Algorithm 1 consists of four steps.

Step 1: Whenever $t = t_k$, a pair of agents is selected and it is monitored whether Assumption 6 is satisfied. Here, t_k , $k = 1, 2, \dots$, indicate predetermined periodic instants executing the goal assignment algorithm. It should be stressed that t_k is selected regardless of the control sampling time [23].

Step 2: If the assumption is correct, temporary variables $\check{\mathcal{N}}_\alpha$, $\check{\mathcal{N}}_\beta$, $\check{\mathcal{N}}_m$, \check{p}_α^* , and \check{p}_β^* under the exchanged goals of agent α and agent β are defined where $m \in \check{\mathcal{N}}_{\alpha\cup\beta}(t_k^-)$; $\check{\mathcal{N}}_{\alpha\cup\beta}(t_k^-) \triangleq \bar{\mathcal{N}}_\alpha(t_k^-) \cup \bar{\mathcal{N}}_\beta(t_k^-) - \{\alpha\} - \{\beta\}$ and $t_k^- \triangleq \lim_{\varepsilon \rightarrow 0^+} t_k - \varepsilon$. Since the neighbors of agents α and β will be updated along with the goal exchange and the communication among agents is undirected, it is necessary to take account of $\bar{\mathcal{N}}_m$ and $\check{\mathcal{N}}_m$. According to the following rules

$$\begin{aligned} \check{\mathcal{N}}_\alpha &= \begin{cases} \bar{\mathcal{N}}_\beta(t_k^-) - \{\alpha\} + \{\beta\}, & \text{if } \alpha \in \bar{\mathcal{N}}_\beta(t_k^-), \\ \bar{\mathcal{N}}_\beta(t_k^-), & \text{if } \alpha \notin \bar{\mathcal{N}}_\beta(t_k^-), \end{cases} \\ \check{\mathcal{N}}_\beta &= \begin{cases} \bar{\mathcal{N}}_\alpha(t_k^-) - \{\beta\} + \{\alpha\}, & \text{if } \beta \in \bar{\mathcal{N}}_\alpha(t_k^-), \\ \bar{\mathcal{N}}_\alpha(t_k^-), & \text{if } \beta \notin \bar{\mathcal{N}}_\alpha(t_k^-), \end{cases} \\ \check{p}_\alpha^* &= p_\beta^*(t_k^-), & \check{p}_\beta^* &= p_\alpha^*(t_k^-), \end{aligned} \quad (12)$$

we get $\check{\mathcal{N}}_\alpha$, $\check{\mathcal{N}}_\beta$, \check{p}_α^* , and \check{p}_β^* . From $\check{\mathcal{N}}_\alpha$ and $\check{\mathcal{N}}_\beta$, $\check{\mathcal{N}}_m$ are determined using the bidirectional edges in the control graph $\bar{\mathcal{G}}(t)$.

Step 3: Two compounded errors e_{cur} and e_{new} are computed where e_{cur} indicates a sum of the local errors under the current goals p_α^* and p_β^* and e_{new} denotes a sum of the errors under the new goals \check{p}_α^* and \check{p}_β^* . Here, $\check{e}_{\alpha,j}$ and $\check{e}_{\beta,j}$ with $j = 1, 2$ are defined as

$$\begin{aligned}\check{e}_{\alpha,1} &= p_\alpha(t_k^-) - \hat{p}_{\alpha,0}(t_k^-) - \check{p}_\alpha^*, & \check{e}_{\alpha,2} &= v_\alpha(t_k^-) - \check{\zeta}_\alpha, \\ \check{e}_{\beta,1} &= p_\beta(t_k^-) - \hat{p}_{\beta,0}(t_k^-) - \check{p}_\beta^*, & \check{e}_{\beta,2} &= v_\beta(t_k^-) - \check{\zeta}_\beta,\end{aligned}$$

where

$$\check{\zeta}_\alpha = -k_{\alpha,1}\check{e}_{\alpha,1} + \hat{v}_{\alpha,0}(t_k^-), \quad \check{\zeta}_\beta = -k_{\beta,1}\check{e}_{\beta,1} + \hat{v}_{\beta,0}(t_k^-).$$

Step 4: If the exchanging condition $e_{cur} > e_{new}$ is satisfied, the two goals are swapped by updating $\bar{\mathcal{N}}_\alpha(t)$, $\bar{\mathcal{N}}_\beta(t)$, $\bar{\mathcal{N}}_m(t)$, $p_\alpha^*(t)$ and $p_\beta^*(t)$ as the temporary variables $\check{\mathcal{N}}_\alpha$, $\check{\mathcal{N}}_\beta$, $\check{\mathcal{N}}_m$, \check{p}_α^* , and \check{p}_β^* , respectively and t_k is recorded as a new exchanging moment τ_g . There updated information holds until the next goal exchange occurs.

Our main result is summarized by the following theorem.

Theorem 1. *Consider multi-agent systems controlled by the backstepping control law (6) and (7) with the estimator (2) under Assumptions 1–5. If there exists a pair of agents satisfying Assumption 6 and there exist τ_g such that $e_{cur}(\tau_g) > e_{new}(\tau_g)$ for $g = 1, 2, \dots$, the leader-following formation control performance can be improved with properly assigned goal positions according to Algorithm 1.*

Proof: Firstly, let us assume that agents α and β swap their goals at $t = \tau_1$. Then, along their current goals and the new (i.e., exchanged) goals, two different Lyapunov function candidates $V_{cur,1}(t)$ and $V_{new,1}(t)$ are defined as follows:

$$\begin{aligned}V_{cur,1}(t) &= \frac{1}{2}(\|p_\alpha(t) - \hat{p}_{\alpha,0}(t) - p_\alpha^*\|^2 + \|v_\alpha(t) - \zeta_\alpha(t)\|^2 \\ &\quad + \|p_\beta(t) - \hat{p}_{\beta,0}(t) - p_\beta^*\|^2 + \|v_\beta(t) - \zeta_\beta(t)\|^2) + \bar{V}_{cur,1}(t) \\ V_{new,1}(t) &= \frac{1}{2}(\|p_\alpha(t) - \hat{p}_{\alpha,0}(t) - \check{p}_\alpha^*\|^2 + \|v_\alpha(t) - \check{\zeta}_\alpha(t)\|^2 \\ &\quad + \|p_\beta(t) - \hat{p}_{\beta,0}(t) - \check{p}_\beta^*\|^2 + \|v_\beta(t) - \check{\zeta}_\beta(t)\|^2) + \bar{V}_{new,1}(t)\end{aligned}\tag{13}$$

Here, $\bar{V}_{cur,1}(t)$ and $\bar{V}_{new,1}(t)$ indicate the remaining terms. Since the continuity of the states (i.e., $p_i(t)$ and $v_i(t)$) and estimated leader information (i.e., $\hat{p}_{i,0}(t)$, $\hat{v}_{i,0}(t)$, and $\hat{u}_{i,0}(t)$) is preserved when the goals are swapped, it holds that $\bar{V}_{cur,1}(\tau_1) = \bar{V}_{new,1}(\tau_1)$. Then, from the definitions of e_{cur} and e_{new} and the exchanging condition in Algorithm 1, it leads to $V_{cur,1}(\tau_1) > V_{new,1}(\tau_1)$.

Now, we will show that $V_{cur,1}(t) > V_{new,1}(t)$ for $t \geq \tau_1$. Even if the goals are exchanged, the dynamics of the error surfaces in (9) is not changed. Thus, the

Algorithm 1: Distributed Goal Assignment Algorithm

input : $t_k, \alpha, \beta, \bar{N}_\alpha(t_k^-), \bar{N}_\beta(t_k^-), \bar{N}_m(t_k^-), p_\alpha^*(t_k^-), p_\beta^*(t_k^-)$ ($m \in \bar{N}_{\alpha \cup \beta}(t_k^-)$)
output: $\tau_g, \bar{N}_\alpha(t), \bar{N}_\beta(t), \bar{N}_m(t), p_\alpha^*(t), p_\beta^*(t)$ ($t \geq t_k$)

- 1 **if** *Assumption 6 holds for agents α and β* **then**
- 2 Define $\check{N}_\alpha, \check{N}_\beta, \check{N}_m, \check{p}_\alpha^*$, and \check{p}_β^* under the exchanged goals of agent α and agent β ;
- 3 Compute $e_{cur} \leftarrow \sum_{j=1}^2 (\|e_{\alpha,j}(t_k^-)\|^2 + \|e_{\beta,j}(t_k^-)\|^2)$ and
 $e_{new} \leftarrow \sum_{j=1}^2 (\|\check{e}_{\alpha,j}\|^2 + \|\check{e}_{\beta,j}\|^2)$;
- 4 **if** $e_{cur} > e_{new}$ **then**
- 5 $\tau_g \leftarrow t_k; g \leftarrow g + 1; k \leftarrow k + 1$; Update $\bar{N}_\alpha(t), \bar{N}_\beta(t), \bar{N}_m(t), p_\alpha^*(t),$
 $p_\beta^*(t)$ as $\bar{N}_\alpha(t) \leftarrow \check{N}_\alpha, \bar{N}_\beta(t) \leftarrow \check{N}_\beta, \bar{N}_m(t) \leftarrow \check{N}_m, p_\alpha^*(t) \leftarrow \check{p}_\alpha^*,$
 $p_\beta^*(t) \leftarrow \check{p}_\beta^*$;
- 6 **end**
- 7 **else**
- 8 $k \leftarrow k + 1$; Keep $\bar{N}_\alpha(t), \bar{N}_\beta(t), \bar{N}_m(t), p_\alpha^*(t), p_\beta^*(t)$
- 9 **end**
- 10 **end**
- 11 **else**
- 12 $k \leftarrow k + 1$; Keep $\bar{N}_\alpha(t), \bar{N}_\beta(t), \bar{N}_m(t), p_\alpha^*(t), p_\beta^*(t)$
- 13 **end**

error surfaces under the current goals and those under the new goals exponentially converge to zero with different initial values but with same speed regarding to the control gains. Therefore, from (13), $V_{cur,1}(t)$ and $V_{new,1}(t)$ have same convergence speed for $t \geq \tau_1$. Owing to $V_{cur,1}(\tau_1) > V_{new,1}(\tau_1)$, the inequality $V_{cur,1}(t) > V_{new,1}(t)$ is guaranteed for $t \geq \tau_1$. Applying this property recursively, we have

$$V_{cur,g}(t) > V_{new,g}(t), \quad t \geq \tau_g. \quad (14)$$

where $g = 1, 2, \dots$.

Let the Lyapunov function $V(t)$ be

$$V(t) = \begin{cases} V_{cur,1}(t), & t \in [t_0, \tau_1) \\ V_{cur,2}(t), & t \in [\tau_1, \tau_2) \\ V_{cur,3}(t), & t \in [\tau_2, \tau_3) \\ \vdots & \vdots \end{cases} \quad (15)$$

Note that $V_{cur,g}(t) = V_{new,g-1}(t)$. Then, we can conclude that

$$V(0) > V(\tau_1) > V(\tau_2) > \dots \quad (16)$$

This implies that the proposed strategy improves the leader-following formation control performance since a discrete jump to a lower value of the Lyapunov function happens whenever the goals are exchanged. ■

Remark 4. In the previous goal assignment algorithm in [24], the assignment condition is defined as $e_{cur} > e_{new}$ where

$$\begin{aligned} e_{cur} &= \|p_\alpha(t_k^-) - p_0(t_k^-) - p_\alpha^*(t_k^-)\|^2 + \|v_\alpha(t_k^-) - \zeta_\alpha(t_k^-)\|^2 \\ &\quad + \|p_\beta(t_k^-) - p_0(t_k^-) - p_\beta^*(t_k^-)\|^2 + \|v_\beta(t_k^-) - \zeta_\beta(t_k^-)\|^2, \\ e_{new} &= \|p_\alpha(t_k^-) - p_0(t_k^-) - \check{p}_\alpha^*\|^2 + \|v_\alpha(t_k^-) - \check{\zeta}_\alpha\|^2 \\ &\quad + \|p_\beta(t_k^-) - p_0(t_k^-) - \check{p}_\beta^*\|^2 + \|v_\beta(t_k^-) - \check{\zeta}_\beta\|^2. \end{aligned} \quad (17)$$

Here, $\check{p}_\alpha^* = p_\beta^*(t_k^-)$ and $\check{p}_\beta^* = p_\alpha^*(t_k^-)$. From the above equations, one can see that the errors depend on the leader's position $p_0(t)$ and velocities $v_0(t)$ used in the virtual controllers. Besides, the leader's acceleration $u_0(t)$ is also used in the local actual controller of each follower. Thus, the implicit assumption in [24] is that all followers have access to the leader but it is not valid in a general distributed network (see Fig. 2(b)). Compared with [24], the pros and cons of the proposed assignment algorithm are summarized as follows.

Pros: (i) The proposed assignment algorithm can be implemented for multi-agent systems with limited leader information under distributed network; and (ii) employing the estimated leader information $\hat{p}_{i,0}(t)$ and $\hat{v}_{i,0}(t)$ from the distributed estimator (2), a local controller and assignment condition are derived and the enhancement of the distributed control performance is rigorously analyzed in the sense of Lyapunov (see the proof of Theorem 1).

Cons: (i) The computation for the estimator (2) and the transmission of the estimated signals (i.e., $\hat{p}_{i,0}$, $\hat{v}_{i,0}$, $\hat{u}_{i,0}$) among agents are necessary; and (ii) to implement the proposed distributed assignment algorithm, a pair of agents needs to know each other's neighbors (i.e., Assumption 6 should be satisfied).

Remark 5. In the recent goal assignment study [24], the structure of the error surfaces are similar to ours and the analysis showing that $V(t)$ decreases whenever the goals are swapped was given similarly (see the proof of Theorem 2 in [24]). In spite of these similarities, the goal assignment strategy in [24] cannot be extended to solve our problem because the only update of the goals in the assignment procedure in [24] may lose the connectivity because of the limited communication range. In order to preserve the connectivity while exchanging goals, we update not only the goals but also the neighbors in the proposed assignment algorithm (see $\bar{\mathcal{N}}_\alpha(t)$, $\bar{\mathcal{N}}_\beta(t)$, $\bar{\mathcal{N}}_m(t)$ in Algorithm 1). This is the main different part from [24] in terms of goal assignment.

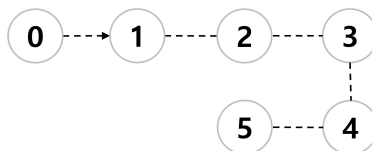


Figure 4: Initial control graph $\bar{\mathcal{G}}(0)$ for Example 1

5. Simulation results

Two examples are simulated to validate the proposed distributed goal assignment strategy where a numerical example and a multi-quadrotor system are considered in the first and second examples, respectively. In this simulation, the formation control results with and without goal assignment will be compared.

Example 1: In this example, one leader and five followers in \mathbb{R}^2 are considered. The initial control graph for the leader and followers is given in Fig. 4. The target

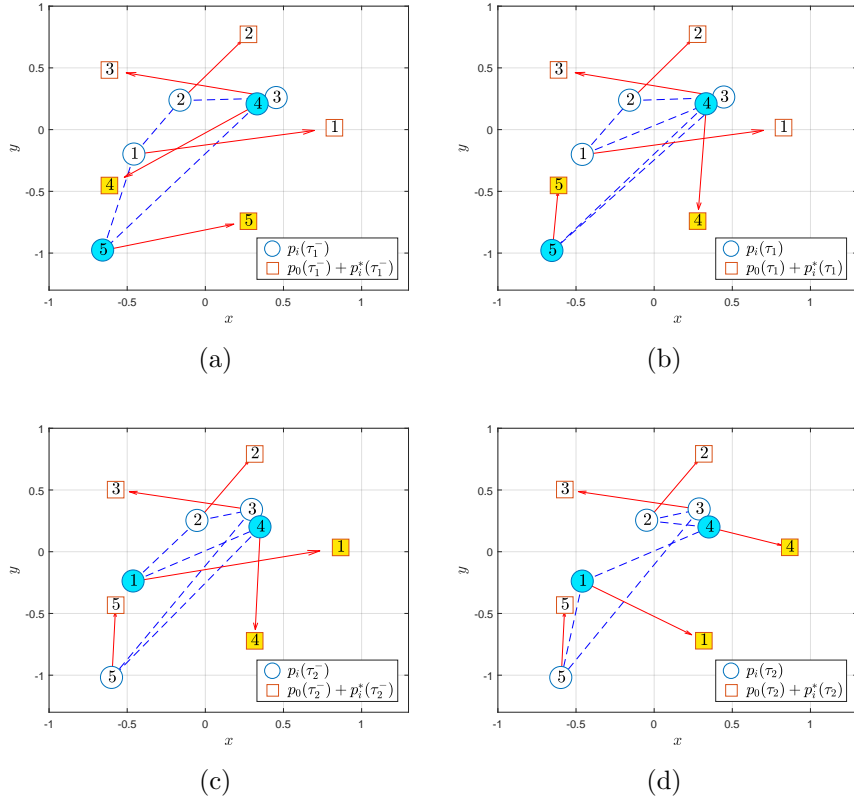


Figure 5: Followers' positions and assigned goals for Example 1 at the exchanging instants (a) $t = \tau_1^-$ (b) $t = \tau_1$ (c) $t = \tau_2^-$ (d) $t = \tau_2$.

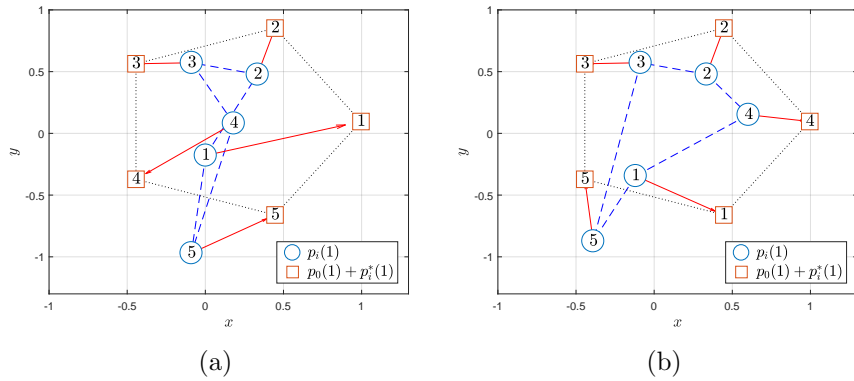


Figure 6: Followers' positions and assigned goals at $t = 1s$ for Example 1 (a) without goal assignment (b) with goal assignment.

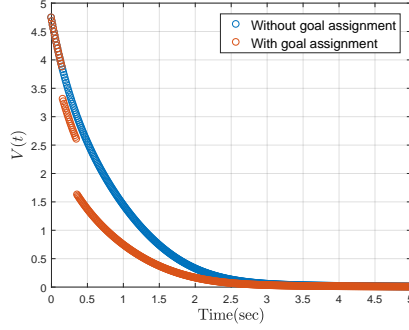


Figure 7: Comparison of the Lyapunov function $V(t)$ for Example 1.

shape is chosen as a pentagon and the initially assigned goals are $p_i^*(0) = G_i$ for $i = 1, \dots, 5$ with

$$\begin{aligned} G_1 &= [0.796, 0]^\top, & G_2 &= [0.246, 0.757]^\top, & G_3 &= [-0.644, 0.468]^\top, \\ G_4 &= [-0.644, -0.468]^\top, & G_5 &= [0.246, -0.757]^\top. \end{aligned}$$

The initial positions and velocities of the followers are randomly chosen. Leader is given by $p_0(t) = [0.2t, 0.2 \sin(t/2)]^\top$ and the followers are set to communicate with nearby followers within the communication range $R = 2$. The controller and estimator gains are selected as $k_{i,1} = 0.5$, $k_{i,2} = 1$, $\gamma_{i,1} = \gamma_{i,2} = 100$, and $\gamma_{i,3} = 20$ where $i = 1, \dots, 5$.

During the simulation, the goal exchange occurs two times with $\tau_1 = 0.15\text{s}$ and $\tau_2 = 0.35\text{s}$ and its progress is described in Fig. 5. In this figure, the blue circles indicate the current positions of the five followers (i.e., $p_i(t)$) and the orange rectangles are the sum of the leader positions and goal positions (i.e., $p_0(t) + p_i^*(t)$). The red solid arrows in these figures are drawn to show which goal is assigned to each follower and the blue dashed lines represent the edges of the control graph $\bar{\mathcal{G}}_F(t)$. Additionally, colored circles and rectangles are for the positions of the followers and their goals to be exchanged, respectively. From Figs. 5(a) and 5(a), it is captured that the goals of followers 4 and 5 are exchanged at $t = \tau_1$. It should be emphasized that not only the assigned goals but also the control graph is changed. Similarly at $t = \tau_2$, the goal exchange between followers 1 and 4 happens in Figs. 5(c) and 5(d).

The comparison of the formation control results at $t = 1\text{s}$ is given in Fig. 6. As the goals are swapped, the goal positions and the edges regarding to $\bar{\mathcal{G}}_F(t)$ in Fig. 6(b) are different from Fig. 6(a). In these figures, the black dotted lines are drawn to visualize the target shape. Note that the formation formed by the followers is relatively closer to the pentagon with goal exchange in Fig. 6(b) than that without

goal assignment in Fig. 6(a). This reveals that the transient formation control performance is enhanced by the proposed assignment strategy. We can see also the performance improvement from Fig. 7 where the blue line is the Lyapunov function $V(t)$ without goal assignment and the orange one is $V(t)$ with goal assignment. As we discussed in the proof of Theorem 1, there exist discrete jumps of $V(t)$ holding $V(\tau_g^-) > V(\tau_g)$ with $g = 1, 2$ and $V(t)$ with goal assignment is always lower than that without goal assignment. From these figures, it appears that the proposed goal assignment strategy provides a performance enhancement of the leader-following formation control.

Example 2: As the second example, 3D formation problem of multiple quadrotors is addressed. A simplified model of the i th quadrotor can be modeled as [32]

$$\begin{aligned}
\ddot{x}_i &= \frac{1}{m}(\cos \phi_i \sin \theta_i \cos \psi_i + \sin \phi_i \sin \psi_i)U_{z,i}, \\
\ddot{y}_i &= \frac{1}{m}(\cos \phi_i \sin \theta_i \sin \psi_i - \sin \phi_i \cos \psi_i)U_{z,i}, \\
\ddot{z}_i &= -g + \frac{1}{m} \cos \phi_i \cos \theta_i U_{z,i}, \\
\ddot{\phi}_i &= a_1 \dot{\theta}_i \dot{\psi}_i + b_1 U_{\phi,i}, \\
\ddot{\theta}_i &= a_2 \dot{\phi}_i \dot{\psi}_i + b_2 U_{\theta,i}, \\
\ddot{\psi}_i &= a_3 \dot{\phi}_i \dot{\theta}_i + b_3 U_{\psi,i},
\end{aligned} \tag{18}$$

where $a_1 = (I_{yy} - I_{zz})/I_{xx}$, $a_2 = (I_{zz} - I_{xx})/I_{yy}$, $a_3 = (I_{xx} - I_{yy})/I_{zz}$, $b_1 = d/I_{xx}$, $b_2 = d/I_{yy}$, and $b_3 = 1/I_{zz}$. The translational and rotational motions of the quadrotors in three directions are assured by (x_i, y_i, z_i) and $(\theta_i, \phi_i, \psi_i)$, respectively. Here, m is the total mass of the system, g indicates the gravitational acceleration, I_{xx} , I_{yy} , and I_{zz} denote the rotary inertia, $U_{z,i}$ is the total thrust, $U_{\phi,i}$, $U_{\theta,i}$, and $U_{\psi,i}$ are the moment. The system parameters are given in Table 1.

Table 1: Quadrotor parameters

| Parameter | Unit | Value |
|-----------|-------------------|-----------|
| g | m/s ² | 9.81 |
| m | kg | 0.486 |
| I_{xx} | kg·m ² | 3.827e-3 |
| I_{yy} | kg·m ² | 3.827e-3 |
| I_{zz} | kg·m ² | 7.6566e-3 |
| d | m | 0.1 |

By defining virtual translational inputs $u_{x,i}$, $u_{y,i}$, $u_{z,i}$ as $u_{x,i} = (1/m)(\cos \phi_i \sin \theta_i \cos \psi_i + \sin \phi_i \sin \psi_i)U_{z,i}$, $u_{y,i} = (1/m)(\cos \phi_i \sin \theta_i \sin \psi_i - \sin \phi_i \cos \psi_i)U_{z,i}$, $u_{z,i} =$

$-g+(1/m) \cos \phi_i \cos \theta_i U_{z,i}$, respectively, the translational subsystem becomes a double integrator system as follows:

$$\begin{aligned}\ddot{x}_i &= u_{x,i}, \\ \ddot{y}_i &= u_{y,i}, \\ \ddot{z}_i &= u_{z,i}.\end{aligned}\tag{19}$$

For (19), the distributed estimator and backstepping controller in Section 3 are designed and Algorithm 1 is applied. However, since the actual control input of the quadrotor is $U_i = [U_{\phi,i}, U_{\theta,i}, U_{\psi,i}, U_{z,i}]^\top$, a sliding mode control algorithm is adopted for controlling the attitude subsystem as follows:

$$\begin{aligned}U_{\phi,i} &= \frac{1}{b_1}(-a_1 \dot{\theta}_i \dot{\psi}_i - k_{\phi,i} \text{sign}(s_{\phi,i}) - \lambda_{\phi,i}(\dot{\phi}_i - \dot{\phi}_{i,d}) + \ddot{\phi}_{i,d}), \\ U_{\theta,i} &= \frac{1}{b_2}(-a_2 \dot{\phi}_i \dot{\psi}_i - k_{\theta,i} \text{sign}(s_{\theta,i}) - \lambda_{\theta,i}(\dot{\theta}_i - \dot{\theta}_{i,d}) + \ddot{\theta}_{i,d}), \\ U_{\psi,i} &= \frac{1}{b_3}(-a_3 \dot{\phi}_i \dot{\theta}_i - k_{\psi,i} \text{sign}(s_{\psi,i}) - \lambda_{\psi,i}(\dot{\psi}_i - \dot{\psi}_{i,d}) + \ddot{\psi}_{i,d}),\end{aligned}$$

where $k_{\phi,i}$, $k_{\theta,i}$, $k_{\psi,i}$, $\lambda_{\phi,i}$, $\lambda_{\theta,i}$, $\lambda_{\psi,i}$ are control design parameters, $s_{\phi,i}$, $s_{\theta,i}$, and $s_{\psi,i}$ are sliding error surfaces, and $\phi_{i,d}$ and $\theta_{i,d}$ are the desired pitch and roll angles, respectively, which are computed from the virtual translational inputs as follows:

$$\begin{aligned}\phi_{i,d} &= \arctan\left(\cos \theta_d \left(\frac{\sin \psi_{i,d} u_{x,i} - \cos \psi_{i,d} u_{y,i}}{u_{z,i} + g}\right)\right), \\ \theta_{i,d} &= \arctan\left(\frac{\cos \psi_{i,d} u_{x,i} + \sin \psi_{i,d} u_{y,i}}{u_{z,i} + g}\right).\end{aligned}\tag{20}$$

The desired yaw angle $\psi_{i,d}$ can be chosen freely and thus it is set to zero in our simulation. Similarly, the last control input $U_{z,i}$ is derived as

$$U_{z,i} = m \sqrt{u_{x,i}^2 + u_{y,i}^2 + (u_{z,i} + g)^2}.\tag{21}$$

For more information on the quadrotor model and the derivation of $\phi_{i,d}$, $\theta_{i,d}$, and $U_{z,i}$, please see [32]. In addition, the sliding mode controllers $U_{\phi,i}$, $U_{\psi,i}$, and $U_{\theta,i}$ for the attitude subsystem are motivated by [33].

In this example, a total of 14 quadrotors are considered as followers and a leader is given by $p_0 = [10 \sin(t/2) \ 10 \cos(t/2) \ t + 30]^\top$. The system parameters are given in Table 1. Goal positions G_i are set to form a sphere with respect to the leader and are initially assigned to the quadrotors as $p_i^*(0) = G_i$, $i = 1, \dots, 14$. We assume that the quadrotors start from the ground and fly to their goal positions with respect to the leader. The goal positions and the initial conditions of the quadrotors are omitted due to the limitation of paper length. For the distributed leader estimators, backstepping controllers, and the sliding mode attitude controllers, the design parameters are

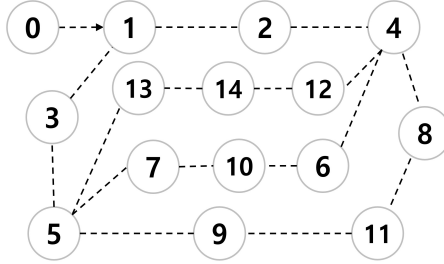


Figure 8: Initial control graph $\bar{\mathcal{G}}(0)$ for Example 2

chosen as $R = 20$, $\gamma_{i,1} = \gamma_{i,2} = 100$, $\gamma_{i,3} = 20$, $k_{i,1} = 0.01$, $k_{i,2} = 5$, $\lambda_{\phi,i} = \lambda_{\theta,i} = \lambda_{\psi,i} = 100$, $k_{\phi,i} = k_{\theta,i} = k_{\psi,i} = 5$ where $i = 1, \dots, 14$.

The initial control graph for the considered multiple quadrotors is given in Fig. 8. According to the proposed assignment strategy, there are eight times of goal exchanging with $\tau_1 = 0.4\text{s}$, $\tau_2 = 0.5\text{s}$, $\tau_3 = 0.8\text{s}$, $\tau_4 = 0.9\text{s}$, $\tau_5 = 1.2\text{s}$, $\tau_6 = 1.3\text{s}$, $\tau_7 = 1.6\text{s}$, and $\tau_8 = 1.9\text{s}$. Fig. 9 shows the followers' positions and their goals at $t = \tau_2$ and $t = \tau_5$. As illustrated in this figure, two goals of a pair of the followers are swapped which leads to the update of the control graph $\bar{\mathcal{G}}(t)$. Fig. 10 captures the quadrotors' positions at $t = 5\text{s}$ with and without goal assignment in xy and xz coordinates. Despite the same initial conditions and design parameters, the quadrotors with the proposed assignment strategy are closer to their goals than without goal assignment. Fig. 11 illustrates the comparison of the Lyapunov functions $V(t)$ where $V(t)$ decreases as the goals are swapped if the proposed assignment algorithm is employed. These figures confirm that the proposed assignment strategy is applicable to the formation control of practical multiple quadrotors.

6. Conclusion

A distributed goal assignment and leader-following formation control problem has been solved for second-order multi-agent systems. Different from the recent goal assignment study, the goal positions of followers are given as relative positions with respect to the leader and the leader information is only available for a small group of the followers. In order to handle the goal assignment problem in leader-following formation control under distributed communication network, a distributed estimator and assignment strategy have been presented. Based on the Lyapunov theory, we have revealed that the assignment strategy improves the control performance while maintaining the closed-loop stability. In addition, the simulation has successfully verified the proposed theoretical result.

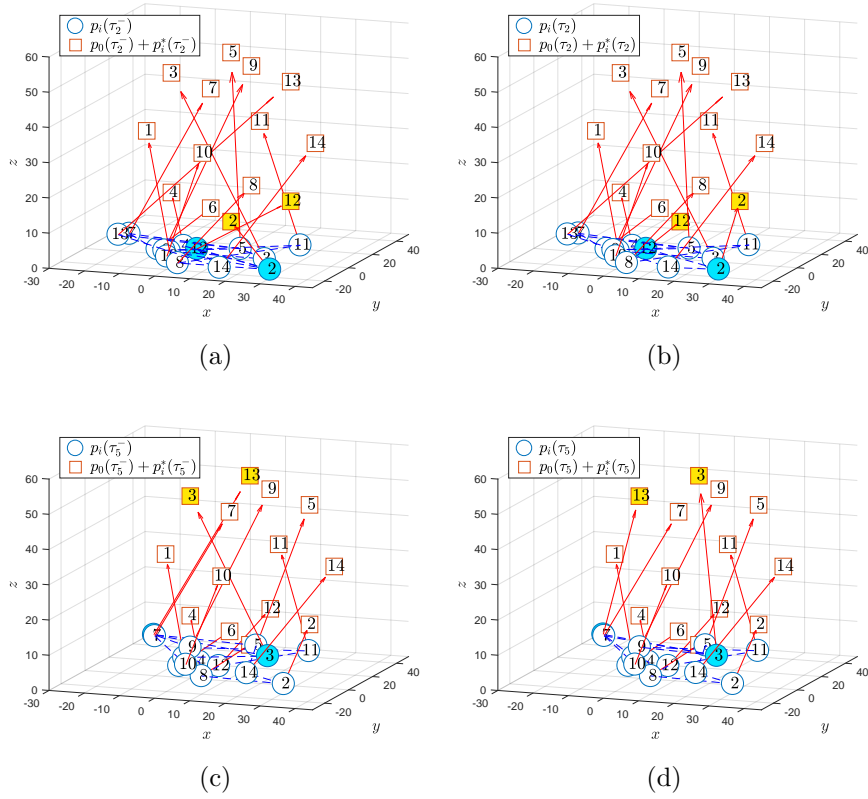


Figure 9: Followers' positions and assigned goals for Example 2 at the exchanging instants (a) $t = \tau_2^-$ (b) $t = \tau_2$ (c) $t = \tau_5^-$ (d) $t = \tau_5$.

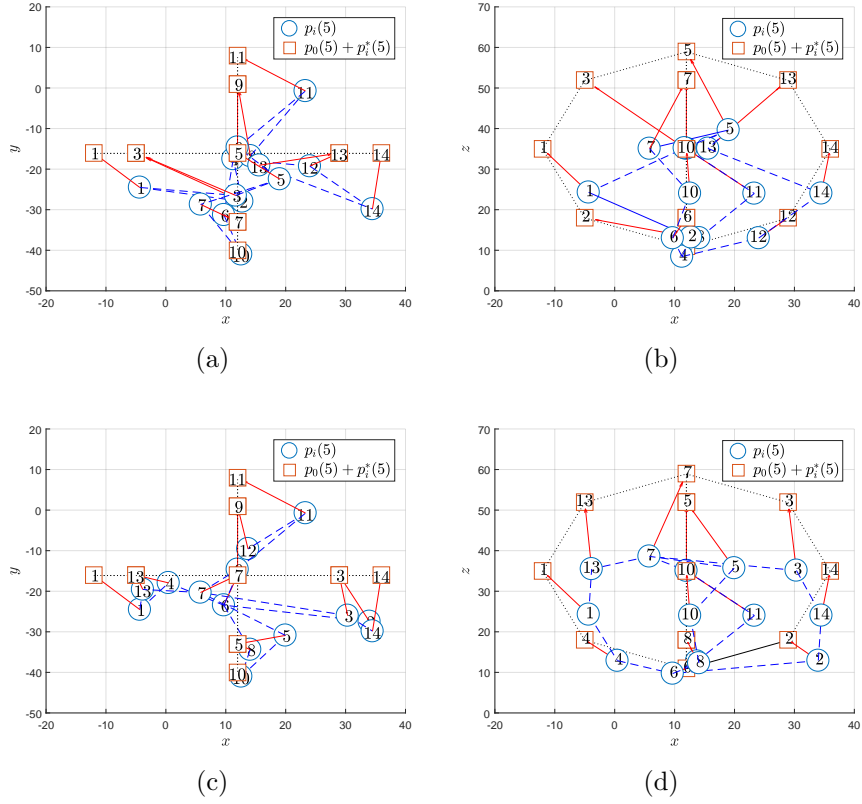


Figure 10: Followers' positions and assigned goals at $t = 5s$ for Example 2 (a) without goal assignment in xy coordinates (b) without goal assignment in xz coordinates (c) with goal assignment in xy coordinates (d) with goal assignment in xz coordinates.

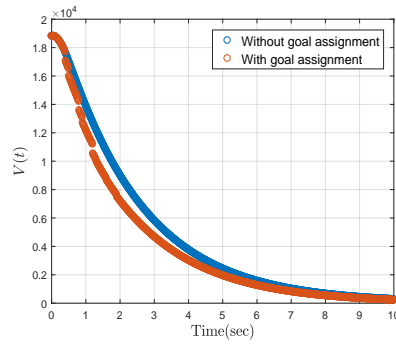


Figure 11: Comparison of the Lyapunov function $V(t)$ for Example 2.

Declaration of Competing Interest

None.

Acknowledgment

This research was supported by the Korea Institute of Science and Technology (KIST) Institutional Program under Grant 2E31581 and by Basic Science Research Program through the National Research Foundation of Korea(NRF) funded by the Ministry of Education(NRF-2021R1A6A3A01086607).

References

- [1] R. Olfati-Saber, J.A. Fax, R.M. Murray, Consensus and cooperation in networked multi-agent systems, *Proc. IEEE* 95 (1) (2007) 215-233.
- [2] W. Ren, R.W. Beard, E.M. Atkins, Information consensus in multivehicle cooperative control, *IEEE Contr. Syst. Magaz.* 27 (2) (2007) 71-82.
- [3] T. Balch, R.C. Arkin, Behavior-based formation control for multirobot teams, *IEEE Trans. Robot. Autom.* 14 (6) (1998) 926-939.
- [4] M.A. Lewis, K.H. Tan, High precision formation control of mobile robots using virtual structures, *Autonom. Robots* 4 (1997) 387-403.
- [5] J. Shao, G. Xie, L. Wang, Leader-following formation control of multiple mobile vehicles, *IET Contr. Theory Appl.* 1 (2) (2007) 545-552.
- [6] K. Shojaei, Neural network formation control of a team of tractor-trailer systems, *Robotica*, 36 (2018) 39-56.
- [7] Z. Gao, G. Guo, Velocity free leader-follower formation control for autonomous underwater vehicles with line-of-sight range and angle constraints, *Inform. Sci.* 486 (2019) 359-378.
- [8] N. Lashkari, M. Biglarbegian, S.X. Yang, Development of a novel robust control method for formation of heterogeneous multiple mobile robots with autonomous docking capability, *IEEE Trans. Auto. Sci., Engin.* 17 (4) (2020) 1759-1776.
- [9] Q. Shi, T. Li, J. Li, C.L.P. Chen, Y. Xiao, Q. Shan, Adaptive leader-following formation control with collision avoidance for a class of second-order nonlinear multi-agent systems, *Neurocomput.* 350 (2019) 282-290.

- [10] H. Kang, W. Wang, C. Yang, Z. Li, Leader-following formation control and collision avoidance of second-order multi-agent systems with time delay, *IEEE Access* 8 (2020) 142571-142580.
- [11] Y. Hua, X. Dong, L. Han, Q. Li, Z. Ren, Finite-time time-varying formation tracking for high-order multiagent systems with mismatched disturbances, *IEEE Trans. Syst., Man, Cybern., Syst.* 50 (10) (2020) 3795-3803.
- [12] R. Wang, X. Dong, Q. Li, Z. Ren, Distributed time-varying formation control for linear swarm systems with switching topologies using an adaptive output-feedback approach, *IEEE Trans. Syst., Man, Cybern., Syst.* 49 (12) (2019) 2664-2675.
- [13] Y. Li, Y. Wu, S. He, Network-based leader-following formation control of second-order autonomous unmanned systems, *J. Frankl. Inst.* 358 (1) (2021) 757-775.
- [14] L. Yan, B. Ma, Adaptive practical leader-following formation control of multiple nonholonomic wheeled mobile robots, *Int. J. Rob. Nonlin. Contr.* 30 (17) (2020) 7216-7237.
- [15] Z. Yan, X. Pan, Z. Yang, L. Yue, Formation control of leader-following multi-UUVs with uncertain factors and time-varying delays, *IEEE Access*, 7 (2019) 118792-118805.
- [16] H. Liu, Y. Wang, F.L. Lewis, Robust distributed formation controller design for a group of unmanned underwater vehicles, *IEEE Trans. Syst., Man, Cybern., Syst.* 51 (2) (2021) 1215-1223.
- [17] C.-D. Liang, M.-F. Ge, Z.-W. Liu, G. Ling, F. Liu, Predefined-time formation tracking control of networked marine surface vehicles, *Contr. Engin. Pract.* 107 (2021) 104682.
- [18] H. Liu, Y. Wang, J. Xi, Completely distributed formation control for networked quadrotors under switching communication topologies, *Syst., Contr. Lett.* 147 (2021) 104841.
- [19] J. Yu, S.M. LaValle, Shortest path set induced vertex ordering and its application to distributed distance optimal formation path planning and control on graphs, in *Proc. 52nd IEEE Conf. Decis. Contr. Firenze, Italy, 2013*, pp. 10-13.

- [20] M. Turpin, K. Mohta, N. Michael, V. Kumar, Goal assignment and trajectory planning for large teams of interchangeable robots, *Auton. Robot* 37 (2014) 401-415.
- [21] D. Panagou, M. Turpin, V. Kumar, Decentralized goal assignment and safe trajectory generation in multirobot networks via multiple Lyapunov functions, *IEEE Trans. Autom. Contr.* 65 (8) (2020) 3365-3380.
- [22] H. Wang, M. Rubenstein, Shape formation in homogeneous swarms using local task swapping, *IEEE Trans. Robot.* 36 (3) (2020) 597-612.
- [23] W. Kowalczyk, Formation control and distributed goal assignment for multi-agent non-holonomic systems, *Applied Sciences* 9 (7) (2019) 1311.
- [24] Y.H. Choi, D. Kim, Goal assignment in leader-following formation control of second-order multi-agent systems. in *Proc. 21st Int. Conf. Contr., Autom., Syst.* Jeju, South Korea, Oct. 12-15, 2021, pp. 1628-1632.
- [25] Y.H. Choi, D. Kim, Distance-based formation control with goal assignment for global asymptotic stability of multi-robot systems, *IEEE Robot. Autom. Lett.* 6 (2) (2021) 2020-2027.
- [26] A. Franchi, P.R. Giordano, Decentralized control of parallel rigid formations with direction constraints and bearing measurements, in *Proc. 51st IEEE Conf. Dec. Contr. Maui, Hawaii, USA, 2012*, pp. 10-13.
- [27] H. Zhang, Z. Li, Z. Qu, F.L. Lewis, On constructing Lyapunov functions for multi-agent systems, *Automatica* 58 (2015) 39-42.
- [28] C.-D. Liang, L. Wang, X.-Yu. Yao, Z.-W., Liu, M.-F. Ge, Multi-target tracking of networked heterogeneous collaborative robots in task space. *Nonlin. Dyn.* 97 (2019) 1159–1173.
- [29] Y. Zhao, Z. Duan, G. Wen, Distributed finite-time tracking of multiple Euler–Lagrange systems without velocity measurements. *Int. J. Robust Nonlin. Contr.* 25 (11) (2015) 1688-1703.
- [30] Z. Zuo, Q.-L. Han, B. Ning, An explicit estimate for the upper bound of the settling time in fixed-time leader-following consensus of high-order multivariable multiagent systems. *IEEE Trans. Indust. Electron.* 66 (8) (2019) 6250-6259.

- [31] M. Krstic, I. Kanellakopoulos, P. Kokotovic, *Nonlinear and Adaptive Control Design*, Hoboken, NJ, Wiley, 1995.
- [32] M. Labbadi, M. Cherkaoui, Robust adaptive backstepping fast terminal sliding mode controller for uncertain quadrotor UAV. *Aerosp. Sci. Techn.* 93 (2019) 105306.
- [33] J.-J.E. Slotine, W. Li, *Applied Nonlinear Systems*, Englewood Cliffs, NJ, Prantice-Hall, 1991.